Available online at www.sciencedirect.com
SCIENCE DIRECT
Journal of Pharmaceutical and Biomedical Analysis 40 (2006) 375–381
JOURNAL OF PHARMACEUTICAL AND BIOMEDICAL ANALYSIS
www.elsevier.com/locate/jpba

Exploration of the direct metabolic effects of mercury II chloride on the kidney of Sprague–Dawley rats using high-resolution magic angle spinning ^{1}H NMR spectroscopy of intact tissue and pattern recognition

Yulan Wang, Mary E. Bollard, Jeremy K. Nicholson, Elaine Holmes *

Biological Chemistry, Biomedical Sciences Division, Faculty of Medicine, Imperial College London, Sir Alexander Fleming Building, South Kensington, London SW7 2AZ, UK

Received 5 April 2005; received in revised form 14 July 2005; accepted 15 July 2005
Available online 16 September 2005

Abstract

Mercury II chloride ($HgCl_2$) toxicity was investigated in Sprague–Dawley rats using high-resolution magic angle spinning (HRMAS) ^{1}H NMR spectroscopy in conjunction with principal component analysis (PCA). Intact renal cortex and papilla samples from Sprague–Dawley rats treated with $HgCl_2$ at two dose levels (0.5 and 2 mg/kg) and from matched controls ($n = 5$ per group) were assessed at 48 h p.d. $HgCl_2$ caused depletion of renal osmolytes such as glycerophosphocholine (GPC), betaine, trimethylamine *N*-oxide (TMAO), *myo*-inositol and taurine in both the renal cortex and the papilla. In addition, relatively higher concentrations of valine, isobutyrate, threonine and glutamate were observed in $HgCl_2$-treated rats, particularly in the renal cortex, which may reflect a counterbalance response to the observed loss of other classes of renal osmolytes. Increased levels of glutamate were present in the cortex of treated rats, which may be associated with $HgCl_2$-induced renal acidosis and disruption of the tricarboxylic acid cycle. A dose response was observed in both cortical and papillary tissue with increasing severity of metabolic disruption in the high dose group. ^{1}H HRMAS NMR profiles of individual animals correlated well with conventional clinical chemistry and histology confirming the reproducibility of the technology and generating complementary molecular pathway information.

Keywords: $HgCl_2$; Principal components analysis; ^{1}H HRMAS NMR spectroscopy; Renal cortex; Renal papilla; Intact tissue; Renal osmolytes

1. Introduction

High-resolution ^{1}H NMR spectroscopy coupled with various of pattern recognition methods have been successfully applied to studying endogenous metabolic changes in biofluids for a wide range of drug toxicity and disease states [1–4]. However, histopathology, which remains the gold standard for evaluating the extent of structural damage, topographical distribution and morphological features, carries no molecular information. We have shown that high-resolution ^{1}H magic-angle-spinning (HRMAS) NMR spectroscopy can provide a metabolic link between histology and metabolite profiles of biofluids, and generates useful metabolic information on small intact tissue samples that can reflect toxicological consequences or mechanisms [5–8]. HRMAS involves spinning tissue samples at high speed at the magic angle ($\theta = 54.7°$). This procedure causes the major line broadening factors such as dipole–dipole interactions, NMR chemical shift anisotropy and magnetic field inhomogeneities to be attenuated, thereby producing ^{1}H NMR spectra of a comparable resolution to those observed in the solution state [9]. ^{1}H HRMAS NMR spectroscopy has been successfully applied to study many types of tissue including liver [5,10], kidney [11] and testis [7] in rats, and a range of human tissues from healthy and diseased populations [12,13]. ^{1}H HRMAS approaches have also

Abbreviations: ALP, alkaline phosphatase; CPMG, Carr-Purcell-Meibom-Gill; FID, free induction decay; GPC, glycerophosphocholine; HRMAS, high-resolution magic angle spinning; NMR, nuclear magnetic resonance; PCA, principal component analysis; TMAO, trimethylamine *N*-oxide; SD, Sprague–Dawley

* Corresponding author. Tel.: +44 20 7594 3195; fax: +44 20 7594 3226.
E-mail address: elaine.holmes@imperial.ac.uk (E. Holmes).

0731-7085/$ – see front matter © 2005 Elsevier B.V. All rights reserved.
doi:10.1016/j.jpba.2005.07.019

been applied to a few toxin studies in experimental animals with toxins including arsenic (As^{3+}) [8], cadmium [14,15] 2-bromoethanamine [6] and thioacetamide [16].

$HgCl_2$ is a potent and well-known model for induction of renal cortical toxicity and targets the S2/S3 portion of the renal proximal tubules of experimental animals [17–20]. $HgCl_2$ impairs the re-absorption function of the proximal tubule, resulting in elevated urinary amino acids and glucose and altering the secretion of hippurate and uric acid [21,22]. Since $HgCl_2$ targets many –SH containing enzymes, the mechanism of action of $HgCl_2$ involves inhibition of mitochondrial succinate and malate dehydrogenase with severe consequential disruption of energy metabolism reflected in the increased urinary excretion of α-ketoglutarate and succinate and decreased excretion of citrate [22]. Augmentation of the renin–angiotensin system exacerbates the degree of renal tubular damage at Hg^{2+} dose levels higher than 1 mg/kg, as renal cortical anoxia is caused by reduced glomerular and tubular blood flow, which contributes to the elevated levels of lactate and creatinine in plasma obtained from animals dosed with high levels of Hg^{2+} [22]. ^{1}H NMR studies of biofluids have shown that toxins that target the S2/S3 region of the renal cortex such as hexachlorobutadiene, uranyl nitrate, *p*-aminophenol and thioacetamide induce similar perturbations in the urinary metabolite profile that are indicative of general renal cortical toxicity [23,24]. Metabolic profiling of $HgCl_2$-treated rats has also been achieved by HPLC–MS and changes in the urinary excretion of metabolites present in relatively low concentrations, such as kynurenic acid, xanthurenic acid, pantothenic acid and 7-methylguanine and a range of sulfated compounds including phenol sulfate and benzene diol sulfate [25] have been found. Depletion of these sulfate compounds in the HPLC–MS profiles was consistent with $HgCl_2$ perturbation of the glutathione pathway.

To date, HRMAS NMR spectroscopy of renal tissue profiles has been used to characterise 2-bromoethanamine hydrochloride [6], cadmium [26], arsenic [8] and thioacetamide [16] toxicity, which with exception of cadmium, do not primarily target the renal proximal tubule. In order to further evaluate HRMAS NMR spectroscopy as a tool for modeling tissue specific lesions, we have chosen $HgCl_2$ as a classic S2/S3 target. ^{1}H HRMAS NMR spectroscopy in combination with principal component analysis (PCA) is employed to investigate the biochemical changes, which occur in the renal cortex and papilla of rats treated with $HgCl_2$ at acutely toxic and sub-toxic doses, with a view to evaluating the role of ^{1}H HRMAS NMR spectroscopy as a pathological probe to directly characterise nephrotoxicity in intact tissue.

2. Experimental details

2.1. Sample details

A single intraperitoneal dose of $HgCl_2$ in saline was administrated to male Sprague–Dawley (SD) rats, aged 6–7 weeks and weighing between 200 and 260 g, at two-dose levels of 0.5 mg/kg ($n = 5$) and 2 mg/kg ($n = 5$). A group of control rats ($n = 5$) were treated with saline only. After sacrifice at 48 h post-dose, samples of renal cortex and papilla were removed from both treated and control animals. All tissue samples were immediately snap frozen and stored at −80 °C. High-resolution ^{1}H HRMAS NMR spectroscopy was subsequently carried out without further extraction as extraction procedures are by nature destructive and multiple extraction procedures are required to obtain the optimal recovery of metabolites present in tissue [27].

2.2. Clinical chemistry and histopathology

The right kidney was dissected free of fat and connective tissue, weighted and processed for histology. Samples of renal and hepatic tissues were fixed in 10% buffered formol saline. After processing wax embedded sections (5 μm) were cut, stained with haematoxylin and eosin and examined by light microscopy. Clinical chemistry assays were performed for serum, alkaline phosphatase (ALP), alanine, aminotransferase, and for urinary glucose and total protein using a Hitachi 917 analyses and appropriate commonly available kits.

2.3. ^{1}H HRMAS NMR spectroscopy

Samples of renal cortex and papilla tissue, each approximately 15 mg, were infused with D_2O and packed into 4 mm zirconia rotors with spherical inserts and Kel-F caps.

All NMR experiments were carried out on a Bruker AV-400 spectrometer operating at a ^{1}H frequency of 400.13 MHz, a temperature of 300 K and a sample-spinning rate of 4 kHz. ^{1}H NMR spectra were recorded using a standard Bruker (Bruker Analytik, Rheinstetten, Germany) high-resolution magic-angle spinning probe with magic-angle gradient. The 90° pulse length was adjusted individually for each sample and ranged between 8.15 and 8.40 μs. For each spectrum 256 transients were collected into 32k data points using a spectral width of 6 kHz and a recycle delay of 2.0 s.

A standard one-dimensional pulse sequence using the first increment of the NOESY pulse sequence for water presaturation [RD–90°–t_1–90°–t_m–90°–ACQ] [28] was employed to suppress the water peak, with irradiation at the water frequency during the recycle delay (RD), and mixing time, t_m of 150 ms. The parameter t_1 was set to 3 μs. An additional spectrum was acquired for each tissue sample using the water-suppressed spin-echo Carr-Purcell-Meibom-Gill (CPMG) pulse sequence [29] to suppress signals from macromolecules and other substances with short T_2 values. A spin–spin relaxation delay ($2n\tau$) of 270 ms was used for all samples and water suppression irradiation was applied during the relaxation delay for 2 s. In order to aid NMR resonance assignments, two-dimensional NMR spectroscopic experiments (COSY and TOCSY) were carried out on selected tissue samples [30].

2.4. Data reduction and pattern recognition

Spectra were phased and baseline-corrected manually using XWINNMR (Bruker Analytik, Rheinstetten, Germany). All free induction decays were multiplied by an exponential function equivalent to a 1 Hz line-broadening factor prior to Fourier transformation. The spectra over the range δ 0.2–10.0 were reduced using AMIX (Bruker Analytik, Rheinstetten, Germany) to 245 regions, each 0.04 ppm wide and the signal intensity in each region was integrated. The region δ 4.5–6.0 was removed to eliminate baseline effects caused by imperfect saturation of the water resonance. Each individual integral region was normalised to the summed integral for each spectrum, prior to pattern recognition analysis. Principal Component Analysis (PCA) was carried out using mean-centered NMR data with the software Simca-P 10.0 (Umetrics, Umeå, Sweden) as a means of data reduction. Data were then visualised using the PC scores plots and loadings plots. Each co-ordinate on the scores plot represents an individual sample and each co-ordinate on the loadings plots corresponds to one NMR spectral region. Thus the loadings plots indicate which spectral regions are responsible for any separation of samples into clusters in the corresponding scores plots [31].

3. Results and discussion

3.1. Clinical chemistry and histopathology

At 48 h p.d, acute renal necrosis was observed in three out of five rats from the low dose group. One animal was reported to have inflammation in the liver. Severe tubular necrosis was observed in all high dose animals. Elevated serum levels of ALP and urinary glucose and protein were observed in two of the five animals in the low dose group and in all of the rats from the high dose group. No abnormalities were reported for any of the control animals.

3.2. Analysis of ^{1}H HRMAS NMR spectra of renal cortical and papillary tissue from control SD rats

No biochemical degradation was observed for any of the tissue samples during NMR experiments. This is consistent with previous studies that have shown that a decrease in the intensities of lipids and TMAO resonances can occur in renal cortex samples after maintaining samples at 303 K for 4 h, but that no change in spectral integrity typically occurred within the duration of measurement used in this study i.e. a total of 30 min at a temperature of 300 K [32]. Typical ^{1}H HRMAS NMR spectra obtained from the renal cortex and papilla from a control rat using the ^{1}H CPMG NMR pulse sequence are shown in Fig. 1. NMR resonances were assigned according to literature values [11] and two-dimensional NMR spectroscopic experiments that were performed on selected samples (data not shown).

Although the spectra acquired for a single tissue region i.e. cortex or papilla were highly consistent, large differences between the biochemical composition of renal cortex and papilla were observed from the NMR spectra of control animals, which is consistent with observations from previous studies [11]. Typical spectra from renal cortical samples contained high levels of lipids, taurine, trimethylamine-*N*-oxide (TMAO), valine, glutamate, lysine, alanine, and *iso*-leucine, whereas the renal papillary spectrum mainly comprised of high levels of renal osmolytes, such as glycerophosphocholine (GPC), betaine and *myo*-inositol, which is also consistent with the study by Garrod et al. [11]. With exception of

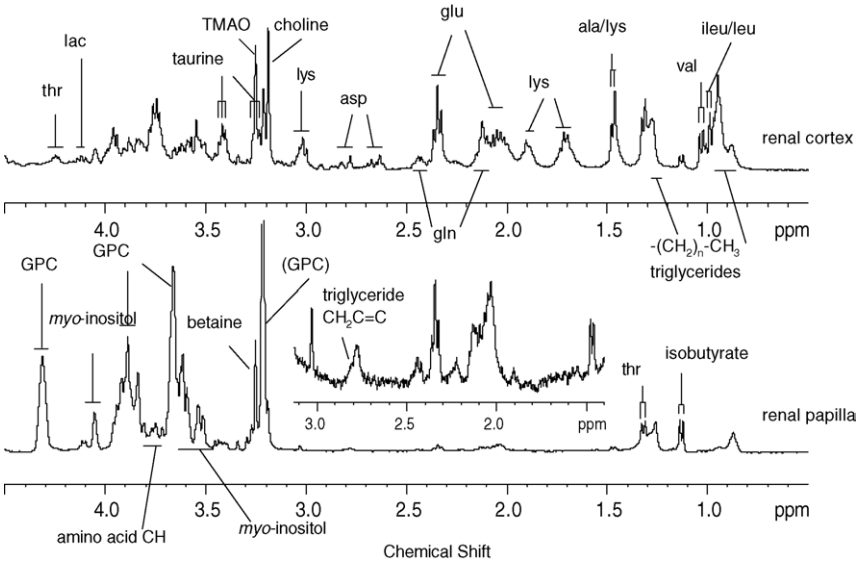

Fig. 1. Four-hundred megahertz HR MAS ^{1}H NMR spectra of renal cortex and renal papilla from a control rat. Spectra are scaled to the baseline noise level, as all samples were comprised of very similar amount of tissues (15 ± 0.2 mg). Abbreviations: asp, aspartate; ala, alanine; gln, glutamine; glu, glutamate; GPC, glycerophosphocholine; ileu, isoleucine; lac, lactate; leu, leucine; lys, lysine; thr, threonine; val, valine.

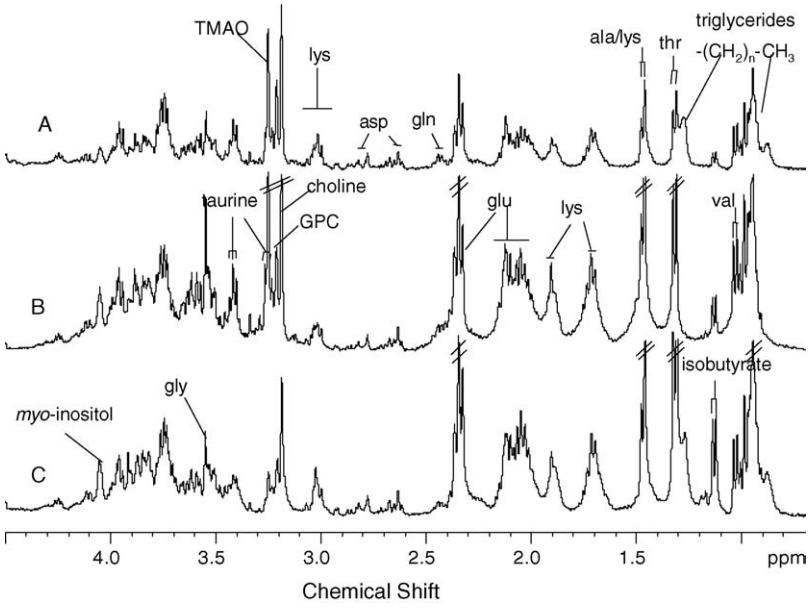

Fig. 2. Typical 400 MHz HRMAS ^{1}H NMR spectra of renal cortex from a rat from the control group (A) and treated with 0.5 mg/kg (B) and 2.0 mg/kg (C) of $HgCl_2$. Abbreviations as for Fig. 1.

TMAO, all renal osmolytes were present in relatively higher concentrations in the renal papilla. GPC, betaine TMAO and *myo*-inositol act as non-perturbing osmoprotective agents and help to ameliorate the denaturating effects of high osmolarity on medullary enzymes [33]. Renal osmolytes occur in high levels in the papilla in order to counterbalance the high urinary concentrations in the loops of Henlé.

3.3. Assessment of the metabolic effects of $HgCl_2$ on the renal cortex

From comparison of the ^{1}H HRMAS NMR spectra of renal cortex from $HgCl_2$-treated rats with matched controls (Fig. 2), a number of differences were observed. Spectra of renal cortical tissues from dosed rats were better resolved than that of control renal cortex. This may be a result of $HgCl_2$-induced damage to the integrity of the proximal tubule cells [34], resulting in a greater percentage of free metabolites in the tissue. It has been observed previously that dosing animals with heavy metals including $HgCl_2$ causes shortening and focal loss of microvilli in the proximal tubule [34]. In addition, isobutyrate and amino acids such as valine, threonine and glutamate were increased in the renal cortex, whilst the resonances from TMAO, taurine and GPC were decreased in intensity. These effects were observed at both dose levels, but were most noticeable in the high dose group. With the exception of one sample from the high dose group, no toxin-related variation in the lipoprotein profile was observed in the standard 1-D spectra. Since the lipoproteins did not play a dominant role in differentiating between control and toxin treated samples, principal components analysis (PCA) was carried out on the ^{1}H CPMG HRMAS after the removal of the sample containing increased triglycerides. NMR spectra of renal cortex from control rats (■), rats treated with $HgCl_2$ at dose level of 2 mg/kg (◯) and 0.5 mg/kg (*) are shown in Fig. 3. Three principal components were calculated for the dataset accounting for 80.1% of the total variation in the data. From the PCA derived scores plot (Fig. 3), the separation of dosed tissue samples from controls was observed in the second PC. The metabolites contributing most to this separation were isobutyrate and amino acids such as valine, threonine, glutamate which were elevated in samples from $HgCl_2$-treated animals and whilst TMAO, taurine and GPC levels were decreased (Table 1). Statistical comparisons of spectra were confirmed by visual analysis of the NMR spectra. A dose response was also evident in the second principal component with clear differentiation between the control and

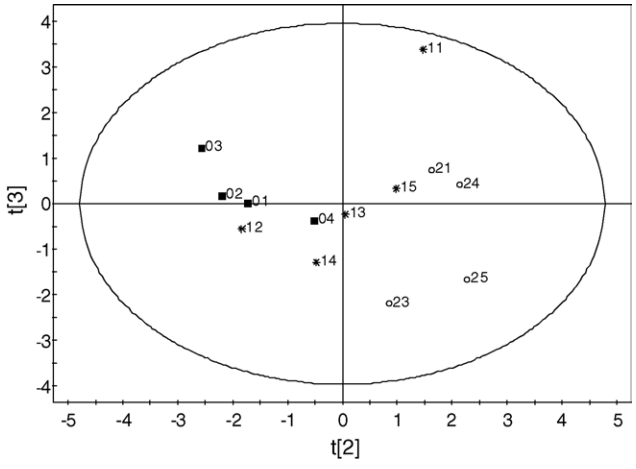

Fig. 3. PC2 vs. PC3 scores plot from PCA of HRMAS ^{1}H NMR spectra of renal cortex from control rats (■) and rats treated with $HgCl_2$ at 0.5 mg/kg (*) and at 2.0 mg/kg (◯).

Table 1
Major observed metabolite changes in rat renal papilla and renal cortex after $HgCl_2$ exposure

Metabolites	Renal papilla		Renal cortex	
	Low dose	High dose	Low dose	High dose
Threonine (1.33 ppm)	–	–	↑	↑↑
Isobutyric acid (1.13 ppm)	↓↓	↓	↑	↑↑
Glutamate (2.0–2.1, 2.34 ppm)	–	↑	↑	↑↑
Alanine (1.47 ppm)	↓↓	–	↑	↑
Lysine (1.89, 1.70, 1.47 ppm)	N/A	N/A	↑	↑↑
Valine (0.98, 1.03 ppm)	–	–	↑	↑
TMAO (3.26 ppm)	N/A	N/A	–	↓
Taurine (3.26, 3.4 ppm)	N/A	N/A	–	↓
GPC (3.22, 4.32 ppm)	↓	↓↓	–	↓
Betaine (3.25, 3.89 ppm)	↓	↓	N/A	N/A
myo-Inositol (4.05 ppm)	↓	↓	–	–

N/A: metabolites not observed. The arrows indicate the direction of the change, i.e. ↓ for decrease and ↑ for increase and number of arrows indicates intensity of change with respect to control tissue.

high dose samples, whilst some overlap occurred between the low dose and the control samples. The low dose samples that were most different in profile from the control samples were those confirmed by the histology and clinical chemical assays to have more severe lesions than the other samples in this group. One of the low dose samples, was differentiated from the other samples in the third principal component. The histology of the renal cortex of this rat was normal but inflammatory changes in the liver were noted. Examination of the loading coefficients indicated that the spectral profile for this animal was dominated by choline which may be a secondary consequence of the hepatic lesion.

Reductions in the concentrations of osmoprotective agents such, taurine and GPC in the cortex is a dominant feature of $HgCl_2$-induced toxicity. This is consistent with the observed metabolic changes after the induction of acute renal cortical toxicity with thioacetamide [16]. The decrease in concentration of renal cortical osmolytes in $HgCl_2$-treated rats was inversely correlated with increased levels of amino acids, which also supports the previous study of thioacetamide-induced renal proximal tubular toxicity [16]. However, whereas TMAO concentrations decreased in the renal cortex of $HgCl_2$-treated rats, an increase in concentration was observed after the administration of thioacetamide and 2-bromoethanamine (primarily a renal medullary toxin with secondary cortical effects), although this observation was noted in spectral profiles at 6–7 h p.d. rather than at 48 h p.d. as measured in the current study. Previous work has shown that the urinary response of TMAO to renal toxicity generally involves an initial elevation in levels (within 24 h p.d.) followed by decreased urinary excretion at later sampling times [35]. Therefore, it is possible that if in the current study (48 h p.d.) TMAO concentrations may have been substantially different at earlier time point respect to the matched control animals.

Many of the characteristic features of ^{1}H NMR urine spectra arise due to the impaired absorption capacity of the proximal tubules and include glucose, amino acids and organic acids. Thus it would be expected that tissue levels of such metabolites would either remain unaltered or decrease. However, in contrast to this assumption, an increase in tissue concentrations of amino acids was observed in the current study. This increase in the relative tissue concentrations of amino acids may be due to disturbed protein synthesis as well as necrosis-induced protein degradation [16]. An alternative explanation may be that the reduction in renal osmolytes observed after treatment of rats with $HgCl_2$ is compensated for by the elevation of amino acids in order to protect the kidney from further injury. Previous studies into $HgCl_2$ toxicity in Neuro-2a cells reported the protective effects of amino acids against cell injury [36]. In another study focusing on renal injury, it was suggested that amino acids act as renal osmolytes against injury and are involved in a process critical for maintaining cellular integrity [37,38].

The increased amounts of glutamate observed in renal cortex of $HgCl_2$-treated rats suggests that exposure to $HgCl_2$ might cause the acid–base equilibrium to shift in the acid direction. Glutamate is a by-product of ammonia (base) synthesis and an increase in glutamate is associated with an increase in the rate of ammonia synthesis [39]. The production of NH_4^+ is needed to neutralise excessive amounts of hydrogen ions in order to maintain acid–base equilibrium. Arguably, high levels of glutamate could also arise from a situation where elevated hydrogen ions are produced by sick animals, which have a reduced food intake, which is known to be the case with $HgCl_2$-treated animals [40]. In this case, fat would be utilised as a major source of energy to produce strong acids such as aceto-acetate, which would dissociate giving rise to hydrogen ions. However, we would expect to observe an increase in concentration of acetate at δ 1.92 in treated rat kidneys compared with control. The fact that an elevation of acetate was not observed in $HgCl_2$ treated kidney samples would imply that $HgCl_2$ may instead cause acidosis in the kidney. $HgCl_2$-induced acidosis has been described previously in $HgCl_2$- and cadmium-treated rats [14,22].

Alternatively, the elevated levels of glutamate in renal cortex samples from $HgCl_2$-treated rats may arise from the inhibition of malate and succinate dehydrogenases causing a

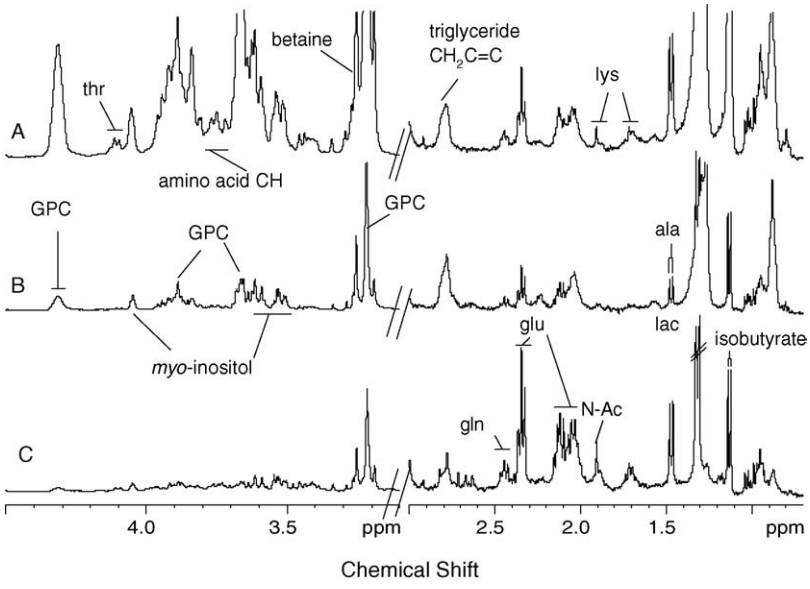

Fig. 4. Four-hundred megahertz HRMAS ^{1}H NMR spectra of renal papilla from a control rat (A) and rats treated with $HgCl_2$ at 0.5 mg/kg (B) and 2.0 mg/kg (C). Abbreviations as for Fig. 1 with the addition of N-Ac, *N*-acetyl glycoprotein fragments.

build up of α-ketoglutarate in the TCA cycle [22]. Glutamate is directly transaminated to give α-ketoglutarate, therefore, glutamate levels could rise in the renal cortex as a result of disruption of the TCA cycle in $HgCl_2$-treated rats.

Care should be taken when investigating metabolic effects of drug and other xenobiotic-induced toxicity as non-specific effects of toxicity such as weight loss due to a reduced food intake may become prominent. It was reported that variations in urinary citrate, α-ketoglutarate, hippurate, creatine are associated with slight weight loss whereas urinary fumarate, glucose, taurine, *N*-methylnicotinamide are associated with more pronounced weight loss [41].

3.4. The effect of $HgCl_2$ on renal papilla

The ^{1}H CPMG HRMAS NMR spectra of renal papilla from $HgCl_2$-treated and control rats are shown in Fig. 4. Several marked changes in the renal papilla were observed after exposure of rats to $HgCl_2$, including decreases in the concentrations of a range of osmoprotective agents such as GPC, betaine and *myo*-inositol. PC analysis of NMR spectra acquired from papilla tissues of control and $HgCl_2$-treated rats at both low (*) and high (◯) doses was carried out (Fig. 5) using the same procedures for the renal cortex. As with the renal cortical data, a clear dose response occurred in PC1. Indeed, on a gross scale the $HgCl_2$-induced changes in the renal papilla were more marked than those observed in the renal cortex. Similar separation was observed from the comparison of control and low dose group although two animals from the low dose group appeared to be very closely associated with the control group. No papillary lesions were reported in the histopathology, however, medullary changes have been reported in other studies as a secondary consequence of $HgCl_2$ toxicity [22]. The separation between control and treated samples was attributed to the depletion of GPC and TMAO, and elevated levels of threonine (δ 1.32), glutamate (δ 2.04, δ 2.12, δ 2.36). Depletion of renal osmolytes in the papilla as a consequence of renal injury has previously been observed in BEA-treated rats [6] exhibiting renal papillary necrosis. It was suggested that the reduction in osmolyte total concentration was due to a homeostatic response to the BEA-induced onset of polyuria, resulting in a decrease in the accumulation of the renal osmolytes [6]. Since $HgCl_2$ is a typical cortical toxin, reduction of osmolytes in renal papilla are likely to be a result of a secondary renal medullary toxicity.

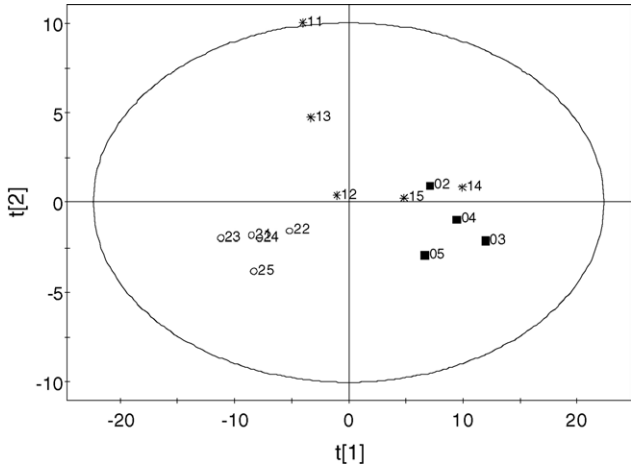

Fig. 5. PC1 vs. PC2 scores plot from PCA of HRMAS ^{1}H NMR spectra of renal papilla from control rats (■) and rats treated with $HgCl_2$ at 0.5 mg/kg (*) and at 2.0 mg/kg (◯).

4. Conclusion

A series of biochemical consequences of $HgCl_2$ administration to rats has been identified using high-resolution magic angle spinning ^1H HRMAS NMR spectroscopy in conjunction with PCA. Consistently depleted concentrations of the renal osmolytes, and elevated concentrations of amino acids were observed in tissues from both the renal cortex and papilla after $HgCl_2$ treatment. These observations are consistent with changes in tissue metabolite profiles observed following the administration of other renal cortical toxins. The observed elevation in amino acid levels may infer an osmoprotective mechanism in response to the general depletion of other classes of osmolytes such as choline derivatives and polyols. Elevated levels of glutamate observed in the cortical and papillary tissues of $HgCl_2$-treated rats compared with controls were attributed to renal tubular acidosis and disruption of the TCA cycle. A strong correlation between the severity of lesion as determined by histology and conventional clinical chemistry and HRMAS profiles was identified. MAS NMR spectroscopic profiling of intact tissue allowed the identification of metabolic indicators of general renal toxicity, such as increased amino acids and depleted osmolytes concentrations, but was also sensitive enough to detect changes that were more specific to $HgCl_2$-induced toxicity including depletion of TMAO and increased levels of lysine and isobutyrate. This work demonstrates that ^1H HRMAS NMR spectroscopy is a viable means of probing molecular information on pathology whilst providing a close correlation with conventional toxicology measures.

Acknowledgements

Oxford Natural Products plc is acknowledged for the funding of Dr. Yulan Wang and we would like to thank the COMET team for providing tissue samples.

References

[1] J.K. Nicholson, D.P. Higham, J.A. Timbrell, P.J. Sadler, Mol. Pharmacol. 36 (1989) 398–404.
[2] M.E. Bollard, E. Holmes, J.C. Lindon, S.C. Mitchell, D. Branstetter, W. Zhang, J.K. Nicholson, Anal. Biochem. 295 (2001) 194–202.
[3] E. Holmes, A.W. Nicholls, J.C. Lindon, S. Ramos, M. Spraul, P. Neidig, S.C. Connor, J. Connelly, S.J.P. Damment, J. Haselden, J.K. Nicholson, NMR Biomed. 11 (1998) 235–244.
[4] C.L. Gavaghan, E. Holmes, E. Lenz, I.D. Wilson, J.K. Nicholson, FEBS Lett. 484 (2000) 169–174.
[5] M.E. Bollard, S. Garrod, E. Holmes, J.C. Lincoln, E. Humpfer, M. Spraul, J.K. Nicholson, Magn. Reson. Med. 44 (2000) 201–207.
[6] S. Garrod, E. Humpher, S.C. Connor, J.C. Connelly, M. Spraul, J.K. Nicholson, E. Holmes, Magn. Reson. Med. 45 (2001) 781–790.
[7] J.L. Griffin, J. Troke, L.A. Walker, R.F. Shore, J.C. Lindon, J.K. Nicholson, FEBS Lett. 486 (2000) 225–229.
[8] J.L. Griffin, L. Walker, R.F. Shore, J.K. Nicholson, Xenobiotica 31 (2001) 377–385.
[9] E.R. Andrew, A. Bradbury, R.G. Eades, Nature 182 (1958) 1659–1661.
[10] Y. Wang, M.E. Bollard, H. Keun, H. Antti, O. Beckonert, T.M. Ebbels, J.C. Lindon, E. Holmes, H. Tang, J.K. Nicholson, Anal. Biochem. 323 (2003) 26–32.
[11] S. Garrod, E. Humpfer, M. Spraul, S.C. Connor, S. Polley, J. Connelly, J.C. Lindon, J.K. Nicholson, E. Holmes, Magn. Reson. Med. 41 (1999) 1108–1118.
[12] L.L. Cheng, C.L. Wu, M.R. Smith, R.G. Gonzalez, FEBS Lett. 494 (2001) 112–116.
[13] L.L. Cheng, C.L. Lean, A. Bogdanova, S.C. Wright, J.L. Ackerman, T.J. Brady, L. Garrido, Magn. Reson. Med. 36 (1996) 653–658.
[14] J.L. Griffin, L.A. Walker, J. Troke, D. Osborn, R.F. Shore, J.K. Nicholson, FEBS Lett. 478 (2000) 147–150.
[15] J.L. Griffin, L.A. Walker, R.F. Shore, J.K. Nicholson, Chem. Res. Toxicol. 14 (2001) 1428–1434.
[16] N.J. Waters, C.J. Waterfield, R.D. Farrant, E. Holmes, J. Nicholson, Chem. Res. Toxicol. (2005).
[17] J.K. Nicholson, M.D. Kendall, D. Osborn, Nature 304 (1983) 633–635.
[18] R.K. Zalups, L.H. Lash, J. Toxicol. Environ. Health 42 (1994) 1–44.
[19] E.M. McDowell, R.B. Nagle, R.C. Zalme, J.S. McNeil, W. Flamenbaum, B.F. Trump, Virchows Arch. B Cell Pathol. 22 (1976) 173–196.
[20] R.C. Zalme, E.M. McDowell, R.B. Nagle, J.S. McNeil, W. Flamenbaum, B.F. Rump, Virchows Arch. B Cell Pathol. 22 (1976) 197–216.
[21] E. Holmes, F.W. Bonner, B.C. Sweatman, J.C. Lindon, C.R. Beddell, E. Rahr, J.K. Nicholson, Mol. Pharmacol. 42 (1992) 922–930.
[22] J.K. Nicholson, J.A. Timbrell, P.J. Sadler, Mol. Pharmacol. 27 (1985) 644–651.
[23] E. Holmes, J.K. Nicholson, A.W. Nicholls, J.C. Lindon, S.C. Connor, S. Polley, J. Connelly, Chemometr. Intell. Lab. 44 (1998) 245–255.
[24] J.P. Shockcor, E. Holmes, Curr. Top. Med. Chem. 2 (2002) 35–51.
[25] E.M. Lenz, J. Bright, R. Knight, I.D. Wilson, H. Major, Analyst 129 (2004) 535–541.
[26] J.L. Griffin, L.A. Walker, R.F. Shore, J.K. Nicholson, Chem. Res. Toxicol. 14 (2001) 1428–1434.
[27] L.L. Cheng, I.W. Chang, D.N. Louis, R.G. Gonzalez, Cancer Res. 58 (1998) 1825–1832.
[28] J.K. Nicholson, P.J.D. Foxall, M. Spraul, R.D. Farrant, J.C. Lindon, Anal. Chem. 67 (1995) 793–811.
[29] S. Meiboom, D. Gill, Rev. Sci. Instrum. 29 (1958) 688–691.
[30] A. Bax, D.G. Davis, J. Magn. Reson. 65 (1985) 355–360.
[31] S. Wold, K. Esbensen, P. Geladi, Chemometr. Intell. Lab. 2 (1987) 37–52.
[32] N.J. Waters, S. Garrod, R.D. Farrant, J.N. Haselden, S.C. Connor, J. Connelly, J.C. Lindon, E. Holmes, J.K. Nicholson, Anal. Biochem. 282 (2000) 16–23.
[33] R.W. Grunewaldt, R.K.H. Kinne, J. Exp. Zool. 283 (1999) 708–724.
[34] C.M. Herak-Kramberger, I. Sabolic, Toxicology 156 (2001) 139–147.
[35] K.P.R. Gartland, F.W. Bonner, J.K. Nicholson, Mol. Pharmacol. 35 (1989) 242–250.
[36] A.J. Becker, E. Mazzio, K.A. Soliman, Faseb. J. 15 (2001) A221.
[37] R.O. Law, D.P.J. Turner, J. Physiol.-London 386 (1987) 45–61.
[38] J.M. Weinberg, M.A. Venkatachalam, R. Garzoquintero, N.F. Roeser, J.A. Davis, Faseb. J. 4 (1990) 3347–3354.
[39] R.J. Harvery, The Kidneys and the Internal Environment, Chapman and Hall, London, 1974, pp. 92–93.
[40] V. Ramalingam, V. Vimaladevi, Asian J. Androl. 4 (2002) 309–311.
[41] S.C. Connor, W. Wu, B.C. Sweatman, J. Manini, J.N. Haselden, D.J. Crowther, C.J. Waterfield, Biomarkers 9 (2004) 156–179.